Journal of Universal Computer Science, vol. 14, no. 14 (2008), 2428-2452
submitted: 30/9/07, accepted: 30/4/08, appeared: 28/7/08 © J.UCS

A Novel Multi-Layer Level Set Method for Image Segmentation

Xiao-Feng Wang
(Intelligent Computing Lab, Hefei Institute of Intelligent Machines
Chinese Academy of Sciences
P.O.Box 1130, Hefei, 230031, China
Department of Automation, University of Science and Technology of China, Hefei 230027
China
Key Lab of Network and Intelligent Information Processing, Department of Computer Science and Technology, Hefei University, Hefei, 230022, China
xfwang@iim.ac.cn)

De-Shuang Huang*
(Intelligent Computing Lab, Hefei Institute of Intelligent Machines
Chinese Academy of Sciences
P.O.Box 1130, Hefei 230031, China
dshuang@iim.ac.cn)

Abstract: In this paper, a new multi-layer level set method is proposed for multi-phase image segmentation. The proposed method is based on the conception of image layer and improved numerical solution of bimodal Chan-Vese model. One level set function is employed for curve evolution with a hierarchical form in sequential image layers. In addition, new initialization method and more efficient computational method for signed distance function are introduced. Moreover, the evolving curve can automatically stop on true boundaries in single image layer according to a termination criterion which is based on the length change of evolving curve. Specially, an adaptive improvement scheme is designed to speed up curve evolution process in a queue of sequential image layers, and the detection of background image layer is used to confirm the termination of the whole multi-layer level set evolution procedure. Finally, numerical experiments on some synthetic and real images have demonstrated the efficiency and robustness of our method. And the comparisons with multi-phase Chan-Vese method also show that our method has a less time-consuming computation and much faster convergence.

Keywords: Curve evolution, Image layer, Level set, Multi-layer, Segmentation, Termination criterion
Categories: G.1.8, I.4.6

1 Introduction

Image segmentation has always been a central problem and complex task in computer vision. Its goal is to change the representation of an image into something that is more meaningful and easier to analyze [Linda, 01]. In other words, it is used to partition a given image into several parts in each of which the intensity is homogeneous. Up to

* The Corresponding Author (dshuang@iim.ac.cn).

now, a wide variety of algorithms and techniques have been developed to solve the image segmentation problem, which often fall into the following categories: thresholding methods, edge-based methods, region-based methods, graph-based methods and model-based methods.

Thresholding methods [Lin, 90], which make decisions based on local pixel information, are effective when the intensity levels of the objects fall squarely outside the range of levels in the background. Due to spatial structural information being ignored, they are effective for simple images that display only small amounts of structure.

Edge-based methods [Palmer, 96] are to focus on edge detection, which is carried out based on the fact that the position of an edge can be obtained by the extreme value of the first-order derivative or zero crossing in the second-order derivative. The main drawback of this kind of segmentation method is that the true boundaries of objects may be divided by noise in the image. Sobel, Robert, and Canny operators are popular examples of edge-based methods [Sonka, 02].

Region-based methods [Chang, 94] usually partition an image into connected regions by grouping neighboring pixels of similar intensity levels. Adjacent regions are then merged under some criterion such as homogeneity and sharpness of region boundaries, etc. The seed region growing, region splitting and region merging approaches are some of the widely used approaches [Adams, 94], [Hijjatoleslami, 98].

Graph-based methods [Urquhart, 82], [Shi, 00] generally represent an image segmentation problem in terms of a graph $G =< V, E >$ where each node $v_i \in V$ corresponds to a pixel in the image, and each edge $e_i \in E$ connects certain pair of neighboring pixels. A weight is associated with each edge based on some property of the pixels that it connects, such as the image intensity. A segmentation S is a partition of V in which each component $C \in S$ corresponds to a connected component in a graph $G' =< V, E' >$, where $E' \subseteq E$.

Model-based methods are usually referred to as the active contour model and the level set method. The main idea of active contour model [Kass, 87], or snake, is to start with a curve around the object to be detected, and the curve moves toward its interior normal and stops on the true boundary of the object based on an energy-minimizing model. The main drawbacks of this method are its sensitivity to initial conditions and the difficulties associated with topological transformations. Since the active contour model was proposed, many methods have been proposed to improve it, in which gradient vector flow and level set are the most important and successful ones.

The gradient vector flow (GVF) method [Xu, 98] generally uses the GVF forces, calculated by applying generalized diffusion equations to both components of the gradient of an image edge map, to drive the snake towards the boundaries of the object. In other words, gradient vector flow method can extend the attractive force near the object boundary to the whole computational region by diffusion. Thus, it expands the capture range of snake so that snake can find objects that are quite far away from the snake's initial position.

Another successful improvement to active contour model is the level set, which has become increasingly popular and been proved to be a useful tool for image segmentation since it was proposed by Osher and Sethian [Osher, 88]. Level set

methods are the ones based on active contours particularly designed to handle the segmentation of deformable structures, which display interesting elastic behaviors, and can handle topological changes. Classical active contour model generally uses spline curves to model the boundary of an object. However, the level set method is to use a deformable curve front for approximating the boundary of an object, whose propagation speed is a function of curvature. In the level set framework, the curve is the iso-contour of a potential function.

Generally, a classical level set method is consist of an implicit data representation of a hypersurface, a set of partial differential equations(PDEs) that govern how the curve moves, and the corresponding numerical solution for implementing this method on computers [Tsai, 05].

It should be mentioned that the early level set methods depend on the gradient of the given image for stopping the evolution of the curve. Therefore, these methods can only detect objects with edges defined by the gradient. Based on the Mumford-Shah functional [Mumford, 89] for segmentation, Chan and Vese [Chan, 01] proposed an easily handled model, or bimodal Chan-Vese model, to detect objects whose boundaries are not necessarily detected by the gradient. This method can partition a given image into two regions, one representing the objects to be detected, and the second one representing the background. Further, they proposed a multi-phase level set framework, also called multi-phase Chan-Vese model [Vese, 02], to segment images with more than two regions. This framework allows one to capture up to 2^n phases of image using n level set functions, i.e., segment the given image into 2^n regions. Generally, the multi-phase Chan-Vese model will evolve more regions than necessary since it assumes that the number of regions is a power of two. In this case, the redundant regions are empty. For example, a 6-phase image requires 3 level set functions, which produce 8 sub-images with 2 ones being empty. Therefore, although this method still gives correct results, it does not have a less time-consuming computation. Furthermore, it usually requires that the initial curves should not overlap each other or be small curves; otherwise, the algorithm may be trapped in a local minimum. Tsai et al [Tsai, 01] proposed a hierarchical method to capture multiple regions which can decrease the computational complexity of the multi-phase Chan-Vese model. The main drawback of this method is the need of user's intervention at each stage of segmentation.

In this paper, we proposed a novel multi-layer level set method that uses only one level set function to solve the multi-phase detection problems. Our multi-layer level set method is based on a kind of conception of image layer and improved numerical solution of bimodal Chan-Vese model. Our proposed method adopts a hierarchical form and does not need user's intervention and re-initialization. Moreover, it can automatically detect each object region after given an initial curve and stop computing in the circumstance that no more object regions can be left in current image layer. Unlike multi-phase Chan-Vese model, it was shown that our method discards unnecessary computations and has a lower computational complexity.

This paper is organized as follows: In Section 2, we briefly introduce the Chan-Vese models and their numerical approximations. Our multi-layer level set method is presented in Section 3. In Section 4, our method is validated by some numerical results on synthetic and real images. Finally, some conclusive remarks are included in Section 5.

2 Chan-Vese Models

The Chan-Vese models are curve evolution implementations of a well-posed case of the Mumford- Shah model [Mumford, 89]. The Mumford-Shah method is an energy-based method introduced by Mumford and Shah via an energy functional in 1989. The basic idea is to find a pair of (u,C) for a given image u_0, where u is a nearly piecewise smooth approximation of u_0, and C denotes the smooth and closed segmenting curve. The general form of the Mumford-Shah functional can be written as:

$$E^{MS}(u,C)=\int_{\Omega}|u_0(x,y)-u(x,y)|^2dxdy+\mu\int_{\Omega\setminus C}|\nabla u(x,y)|^2dxdy+\nu\cdot Length(C), \quad (1)$$

where μ and ν are positive constants, Ω denotes image domain, the curve $C\subset\Omega$. To solve the Mumford-Shah problem is to minimize the functional over u and C. The removal of any of the above three terms in (1) will result in trivial solutions for u and C [Tsai, 01]. However, with all three terms, it becomes a difficult problem to solve since u is a function in an N-dimensional space ($N=2$ in 2D image segmentation), while C is an $N-1$-dimensional data set. The Chan-Vese model is an alternative solution to this problem which solves the minimization of (1) by minimizing the following energy functional:

$$E^{CV}(c_1,c_2,C)=\mu\cdot Length(C)+\nu\cdot Area(inside(C))+\lambda_1\cdot\int_{inside(C)}|u_0(x,y)-c_1|^2dxdy+\lambda_2\cdot\int_{outside(C)}|u_0(x,y)-c_2|^2dxdy, \quad (2)$$

where μ,ν,λ_1 and λ_2 are positive constants, usually fixing $\lambda_1=\lambda_2=1$ and $\nu=0$. c_1 and c_2 are the averages of u_0 inside C and outside C, respectively.

To solve this minimization problem, the level set method [Osher, 88] is used which replaces the unknown curve C by the level-set function $\phi(x,y)$, considering that $\phi(x,y)>0$ if the point (x,y) is inside C, $\varphi(x,y)<0$ if (x,y) is outside (x,y), and $\phi(x,y)=0$ if (x,y) is on C. Thus, the energy functional $E^{CV}(c_1,c_2,C)$ can be reformulated in terms of the level set function $\phi(x,y)$:

$$E_{\varepsilon}^{CV}(c_1,c_2,\phi)=\mu\cdot\int_{\Omega}\delta_{\varepsilon}(\phi(x,y))|\nabla\phi(x,y)|dxdy+\nu\cdot\int_{\Omega}H_{\varepsilon}(\phi(x,y))dxdy$$
$$+\lambda_1\cdot\int_{\Omega}|u_0(x,y)-c_1|^2H_{\varepsilon}(\phi(x,y))dxdy+\lambda_2\cdot\int_{\Omega}|u_0(x,y)-c_2|^2(1-H_{\varepsilon}(\phi(x,y)))dxdy, \quad (3)$$

where $H_{\varepsilon}(z)$ and $\delta_{\varepsilon}(z)$ are the regularized approximation of heaviside function and Dirac delta function, respectively. This minimization problem is solved by taking the Euler-Lagrange equations and updating the level set function $\phi(x,y)$ by the gradient descent method:

$$\frac{\partial \phi}{\partial t} = \delta_\varepsilon(\phi)[\mu div(\frac{\nabla \phi}{|\nabla \phi|}) - \nu - \lambda_1(u_0 - c_1)^2 + \lambda_2(u_0 - c_2)^2], \quad (4)$$

where c_1 and c_2 can be respectively updated at each iteration by:

$$c_1(\phi) = \frac{\int_\Omega u_0(x,y)H(\phi(x,y))dxdy}{\int_\Omega H(\phi(x,y))dxdy} \quad c_2(\phi) = \frac{\int_\Omega u_0(x,y)(1-H(\phi(x,y)))dxdy}{\int_\Omega (1-H(\phi(x,y)))dxdy}. \quad (5)$$

The main advantages of this model are: it automatically detects interior contours, the initial curve can be placed anywhere in the image and it detects both contours with, or without gradient [Chan, 01]. However, as a bimodal model, it is applicable only for images that contain one class of objects. Therefore, Chan and Vese proposed the multi-phase Chan-Vese model for more complex images, in which two or more coupled curves evolve simultaneously to segment images containing multiple classes of objects. Particularly, here we consider a four-phase Chan-Vese model, in which two coupled level set function ϕ_1 and ϕ_2 evolve according to the coupled Euler-Lagrange equations. Suppose that the initial two curves can divide the given image u_0 into four disjoint regions:

$$\begin{aligned} \Omega_{11} &= \{\phi_1 > 0, \phi_2 > 0\} \quad \Omega_{12} = \{\phi_1 > 0, \phi_2 < 0\} \\ \Omega_{21} &= \{\phi_1 < 0, \phi_2 > 0\} \quad \Omega_{22} = \{\phi_1 < 0, \phi_2 < 0\}. \end{aligned} \quad (6)$$

Let C_{11}, C_{12}, C_{21} and C_{22} be the averages of u_0 inside Ω_{11}, Ω_{12}, Ω_{21} and Ω_{22}, respectively.

$$c_{11} = \frac{\int_\Omega u_0(x,y)H(\phi_1)H(\phi_2)dxdy}{\int_\Omega H(\phi_1)H(\phi_2)dxdy} \quad c_{12} = \frac{\int_\Omega u_0(x,y)H(\phi_1)(1-H(\phi_2))dxdy}{\int_\Omega H(\phi_1)(1-H(\phi_2))dxdy}$$

$$c_{21} = \frac{\int_\Omega u_0(x,y)(1-H(\phi_1))H(\phi_2)dxdy}{\int_\Omega (1-H(\phi_1))H(\phi_2)dxdy} \quad c_{12} = \frac{\int_\Omega u_0(x,y)(1-H(\phi_1))(1-H(\phi_2))dxdy}{\int_\Omega (1-H(\phi_1))(1-H(\phi_2))dxdy}. \quad (7)$$

Thus, we can define the associated energy functional without the length term as follows:

$$\begin{aligned} E_4^{CV}(c,\phi) = {} & \nu \cdot \int_\Omega |\nabla H(\phi_1)|dxdy + \nu \cdot \int_\Omega |\nabla H(\phi_2)|dxdy + \int_\Omega |u_0 - c_{11}|^2 H(\phi_1)dxdy \\ & + \int_\Omega |u_0 - c_{12}|^2 H(\phi_1)(1-H(\phi_2))dxdy + \int_\Omega |u_0 - c_{21}|^2 (1-H(\phi_1))H(\phi_2)dxdy \\ & + \int_\Omega |u_0 - c_{22}|^2 (1-H(\phi_1))(1-H(\phi_2))dxdy, \end{aligned} \quad (8)$$

where $c = (c_{11}, c_{12}, c_{21}, c_{22})$ and $\phi = (\phi_1, \phi_2)$.

The evolution of ϕ_1 and ϕ_2 follows the following Euler-Lagrange equations:

$$\frac{\partial \phi_1}{\partial t} = \delta_\varepsilon(\phi_1)[\mu div(\frac{\nabla \phi_1}{|\nabla \phi_1|}) - ((u_0 - c_{11})^2 - (u_0 - c_{21})^2)H(\phi_2) - ((u_0 - c_{12})^2 - (u_0 - c_{22})^2)(1 - H(\phi_2))], \tag{9}$$

$$\frac{\partial \phi_2}{\partial t} = \delta_\varepsilon(\phi_2)[\mu div(\frac{\nabla \phi_2}{|\nabla \phi_2|}) - ((u_0 - c_{11})^2 - (u_0 - c_{21})^2)H(\phi_1) - ((u_0 - c_{12})^2 - (u_0 - c_{22})^2)(1 - H(\phi_1))]. \tag{10}$$

As described in Section 1, this method does not have a less time-consuming computation. As the number of level set function increases, the system of governing equations will become more complicated, and the numerical solution will become more difficult to be obtained because of slow convergence with long iterations.

3 Multi-Layer Level Set Method

To solve the multi-phase image segmentation problem, we proposed the multi-layer level set method. In this Section, we will discuss this new method. Firstly, the conception of image layer and multi-layer is introduced. Then, the initialization method and computational method were given for signed distance function, and Neumann boundary condition was used as the boundary condition of the level set function evolution. Termination criterion was proposed for curve evolving in a certain image layer, and a scheme for accelerating curve evolution process was designed for curve evolution in a queue of sequential image layers. Finally, a termination criterion was proposed for the whole multi-layer level set evolution procedure by detecting background image layer, and then the algorithm steps were presented.

3.1 Image Layer

Assume that a given gray image u_0 contains $(n+1)$ phases, i.e. the given image can be segmented into n classes of object regions and one background region. Here, u_0, or original image layer L_0, can be defined as follows:

$$L_0 = u_0 = \cup_{l=1}^{n}(\Omega_l^1 \cup \Omega_l^2 \cup \cdots \cup \Omega_l^{l_m}) \cup \Omega_{background}, \tag{11}$$

where $\Omega_l^i (l = 1, 2...n, i = 1, 2, ...l_m)$ denotes the *ith* region belonging to the *lth* class of objects, l_m is the number of regions belonging to the *lth* class of objects. $\Omega_l^1 \cup \Omega_l^2 \cup \cdots \cup \Omega_l^{l_m}$ and $\Omega_{background}$ denote the *lth* class of object region and the background region, respectively.

Now, if the $1st$ class of object region $\Omega_1^1 \cup \Omega_1^2 \cup \cdots \cup \Omega_1^{1_m}$ is partitioned from L_0 using a certain image segmentation method, and the intensity of $\Omega_1^1 \cup \Omega_1^2 \cup \cdots \cup \Omega_1^{1_m}$ is replaced by an average of the intensities of outer regions, then the new region is

represented as $\Omega_1^{b1} \cup \Omega_1^{b2} \cup \cdots \cup \Omega_1^{b1_m}$. Thus, a new image layer L_1 which does not contain the 1st class of objects can be formed as follows:

$$L_1 = (\cup_{l=2}^{n}(\Omega_l^1 \cup \Omega_l^2 \cup \cdots \cup \Omega_l^{i_m})) \cup (\Omega_1^{b1} \cup \Omega_1^{b2} \cup \cdots \cup \Omega_1^{b1_m}) \cup \Omega_{background}. \quad (12)$$

Fig.1 illustrates the transformation from L_0 to L_1, where L_0 contains two class of objects , i.e., $\Omega_1^1 \cup \Omega_1^2$ and $\Omega_2^1 \cup \Omega_2^2$, and L_1 contains one class of objects, i.e., $\Omega_2^1 \cup \Omega_2^2$.

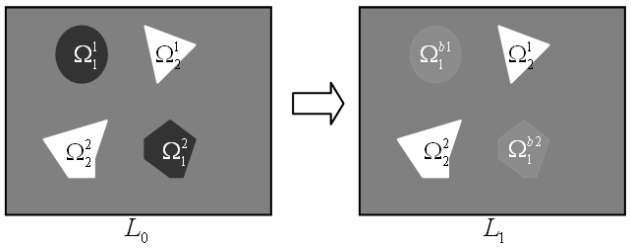

Figure 1: Illustration of transformation from L_0 to L_1.

In the same way, the 2*nd* class of object regions $\Omega_2^1 \cup \Omega_2^2 \cup \cdots \cup \Omega_2^{2_m}$ is partitioned from L_1 and replaced by $\Omega_2^{b1} \cup \Omega_2^{b2} \cup \cdots \cup \Omega_2^{b2_m}$. A new image layer L_2 which does not contain the 1st and 2nd class of objects is then obtained as follows:

$$\begin{aligned} L_2 = (\cup_{l=3}^{n}(\Omega_l^1 \cup \Omega_l^2 \cup \cdots \cup \Omega_l^{i_m})) \cup (\Omega_1^{b1} \cup \Omega_1^{b2} \cup \cdots \cup \Omega_1^{b1_m}) \\ \cup (\Omega_2^{b1} \cup \Omega_2^{b2} \cup \cdots \cup \Omega_2^{b2_m}) \cup \Omega_{background}. \end{aligned} \quad (13)$$

In this manner, L_l which does not contain the 1*st* till the *lth* class of objects can be obtained as follows:

$$L_l = (\cup_{k=l+1}^{n}(\Omega_k^1 \cup \Omega_k^2 \cup \cdots \cup \Omega_k^{k_m})) \cup (\cup_{k=1}^{l}(\Omega_k^{b1} \cup \Omega_k^{b2} \cup \cdots \cup \Omega_k^{bk_m})) \cup \Omega_{background}. \quad (14)$$

Finally, L_n or background image layer $L_{background}$, which does not contain any object, is obtained as follows:

$$L_{background} = L_n = \cup_{l=1}^{n}(\Omega^{b1}{}_l \cup \Omega_l^{b2} \cup \cdots \cup \Omega_l^{bl_m}) \cup \Omega_{background}. \quad (15)$$

Actually, with the implementation of replacing the intensities of segmented object regions by an average of the intensities of outer regions in each image layer, the intensity difference of each image layer decreases gradually. Obviously, the intensity difference of original image layer is largest, and the intensity replacement causes the lowest intensity difference of background image layer. This decreasing trend of the intensity difference is a very important process since it can be used to control the speed of curve evolution.

In this paper, the level set method is selected to segment images. Firstly, the level set curve evolves in original image layer L_0 and splits into several curves according to the topological structure of the 1*st* class of objects. As a result, the evolving process of the curves is stopped on the true boundaries of the 1*st* class of objects. Thus, the partition $\Omega_1^1 \cup \Omega_1^2 \cup \cdots \cup \Omega_1^{1_m}$ is obtained and replaced by $\Omega_1^{b1} \cup \Omega_1^{b2} \cup \cdots \cup \Omega_1^{b1_m}$ to form a new image layer L_1. Then, the curve will continue to evolve in L_2 from the initial position in original image layer L_0. In the same way, a new image layer L_3 is formed. In this manner, we will finally reach the background image layer $L_{background}$ and the curve should stop evolving automatically. Consequently, a queue of sequential image layers is obtained as follows:

$$L_0 \to L_1 \to L_2 \to L_{n-1} \to L_n(L_{background}) . \tag{16}$$

It's easy to draw a conclusion that the 1*st* till the *nth* class of objects can be segmented accordingly from L_0 to L_{n-1}, and nothing can be segmented from the background image layer $L_{background}$. Therefore, the curve should stop evolving in background image layer $L_{background}$ to avoid a long time over-segmentation, and the whole multi-layer level set evolution procedure should be terminated correspondingly.

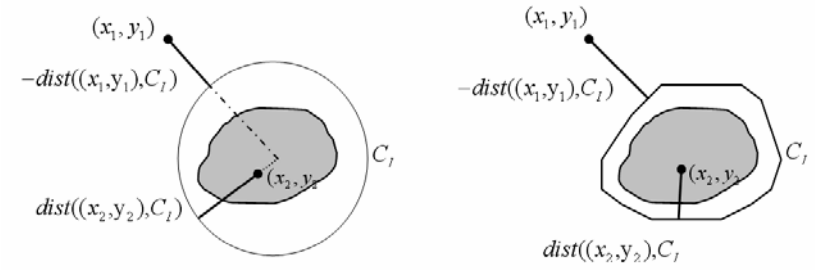

Figure 2: Illustration of computing signed distance function according to different initial curves. (a) Circle-shape closed curve; (b) Irregular-shape closed curve.

3.2 Initialization and Signed Distance Function Computation

In level set method, it is necessary to initialize the level set function as a signed distance function according to initial curve before the evolution as follows:

$$\operatorname{sgn}(\phi(x,y)) = \begin{cases} -dist((x,y),C_I) & \text{if (x,y) is outside } C_I \\ 0 & (x,y) \in C_I \\ dist((x,y),C_I) & \text{if (x,y) is inside } C_I \end{cases}, \tag{17}$$

where C_I is initial closed curve, and $dist((x,y),C_I)$ is the smallest Euclidean distance of (x,y) to the points in C_I. Fig.2 illustrates how to compute sgn($\phi(x,y)$) for different initial curves.

As seen in Fig 2 (b), this step is a time-consuming process for an irregular-shape initial curve since the curve can hardly be parameterized.Therefore, in traditional level set methods, initial curve is often intentionally chosen as an easily parameterized curve such as circle or rectangle. Whereas, in our multi-layer level set method, only one level set function is employed to segment multi-class of objects. To achieve this goal, the initial curve is required to be close to or even touch all objects as much as possible and return to the initial position in original image layer L_0 before the curve evolution starts in each image layer. Obviously, the regular circle or rectangle shape curve satisfying our requirement is inevitably very large so that all objects distributing irregularly can be enclosed. The initialization of level set function is timesaving if these regular initial curves are used. However, on the other hand, a larger initial curve will slow down the curve evolution and sometimes result in the instability of the evolution.Therefore, in this paper we consider using irregular-shape curve as initial curve.Though the initialization becomes a little time-consuming, this process is deserved since it is implemented only once before curve evolution starts in original image layer L_0 and needn't be carried out in later image layers. Most importantly, it can speed up the evolution process and help to gain a stable solution.

Since irregular-shape initial curve C_I can only be represented by singular points set, we should compute the distance $dist((x,y),C_I)$ for every point (x,y) in image. If we directly compute the $dist((x,y),C_I)$, the overall computational complexity will be $O(M\times N)$, where M is the number of singular points of C_I and N is the number of grid points. Using fast marching method, it can be reduced to $O(N\ln M)$ [Malladi, 95]. In this paper, we firstly use fast marching method [Sethian, 96] to construct a sign map S which is used to distinguish whether the point (x,y) is inside or outside the initial curve C. Then, we compute $dist((x,y),C_I)$ using Voronoi source scanning method [Tsai, 02], which can further decrease the overall computational complexity to $O(N)$. Finally, the signed distance function is constructed by multiplying $dist((x,y),C_I)$ by corresponding S_{ij} in S.

For more detailed technical description about fast marching method and Voronoi Source Scanning method, readers can refer to literatures [Sethian, 96] and [Tsai, 02].

3.3 Boundary Condition

In bimodal Chan-Vese model, the curve evolution equation (4) can be obtained by minimizing the energy functional $E^{CV}(c_1,c_2,C)$ with respect to φ with a natural boundary condition:

$$\frac{\delta_\varepsilon(\phi)}{|\nabla\phi|}\frac{\partial\phi}{\partial\vec{n}}=0 \ on\ \partial\Omega, \tag{18}$$

where $\vec{n}$ denotes the exterior normal to the boundary $\partial\Omega$.

In our numerical solution, we choose Neumann boundary condition to replace natural boundary condition in (18) as follows:

$$\frac{\partial \phi}{\partial \vec{n}} = 0 \; on \; \partial\Omega \; . \tag{19}$$

Usually, Neumann boundary condition has many advantages. First, it is easy to implement since there are no values to assign for ϕ at the boundary. Second, it implies that the solution of (4) satisfies a maximum principle. Moreover, the gaps of the curve C may appear only when advancing the zero level set which would change its topology, and cannot come from outside of Ω because of the spurious values created by the Neumann boundary condition. The drawback is that it makes the level set function orthogonal to the boundary that is not always the best way to minimize the energy functional [Allaire, 05].

3.4 Termination Criterion for Curve Evolution in a Single Image Layer

In our multi-layer method, the curve will evolve in each image layer except background image layer. Therefore, we should consider energy minimizing problem in a single image layer. Here, the energy functional of the *lth* image layer L_l can be defined as:

$$\begin{aligned} E_l^{ML}(c_1, c_2, C_l) = \mu \cdot Length(C_l) + \lambda_1 \cdot \int\limits_{inside(C_l)} \left| L_l(x,y) - c_1 \right|^2 dxdy \\ + \lambda_2 \cdot \int\limits_{outside(C_l)} \left| L_l(x,y) - c_2 \right|^2 dxdy \, , \end{aligned} \tag{20}$$

where C_l denotes variable curve in L_l; μ is length parameter. λ_1 and λ_2 are positive constants, usually fixed at $\lambda_1 = \lambda_2 = 1$; c_1 and c_2 are averages of L_l inside C_l and outside C_l, respectively. The energy functional $E_l^{ML}(c_1, c_2, C_l)$ can also be reformulated in terms of the level set function ϕ and a regularization parameter ε:

$$\begin{aligned} E_{l,\varepsilon}^{ML}(c_1, c_2, \phi) = \mu \cdot \int_\Omega \delta_\varepsilon(\phi(x,y)) \left| \nabla \phi(x,y) \right| dxdy + \lambda_1 \cdot \int_\Omega \left| L_l(x,y) - c_1 \right|^2 H_\varepsilon(\phi(x,y)) dxdy \\ + \lambda_2 \cdot \int_\Omega \left| L_l(x,y) - c_2 \right|^2 (1 - H_\varepsilon(\phi(x,y))) dxdy \, , \end{aligned} \tag{21}$$

where $H_\varepsilon(x)$ and $\delta_\varepsilon(x)$ are the regularized approximation of heaviside function $H(z)$ and Dirac delta function $\delta_0(z)$, respectively.

$$H(z) = \begin{cases} 1, & if \; z \geq 0 \\ 0, & if \; z < 0 \end{cases} \; , \; \delta_0(z) = \frac{d}{dz} H(z) \, . \tag{22}$$

Finding the minimum of (21) is done by introducing an artificial time variable $t \geq 0$, and moving φ in the steepest descent direction to a steady state with the initial condition and boundary condition defined in (23b):

$$\frac{\partial \phi}{\partial t} = \delta_\varepsilon(\phi)[\mu div(\frac{\nabla \phi}{|\nabla \phi|}) - \lambda_1(L_l - c_1)^2 + \lambda_2(L_l - c_2)^2], \tag{23a}$$

$$\phi(0, x, y) = \phi_0(x, y) \; in \; \Omega, \quad \frac{\partial \phi}{\partial \vec{n}} = 0 \; on \; \partial\Omega. \tag{23b}$$

Meanwhile, curve, or zero level set function, will split according to the topological structure of object and evolves towards the true boundaries of one class of objects in L_l. When evolving curves finally arrive at the position of true boundaries C_l^*, curves should stop evolving in L_l. The object area filling step is implemented to transform L_l to L_{l+1} by replacing the intensities of object regions by the average of the intensities of outer regions. Then, the curve returns to its initial starting position and continues to evolve in new image layer L_{l+1}. Now, a problem of when and how curves automatically stop evolving in a certain image layer or what termination criterion is for curves evolution is arising.

In bimodal Chan-Vese method, to obtain a global minimizer of (21), $H_\varepsilon(z)$ is chosen as a noncompactly supported smooth strictly monotone approximation of the Heaviside function $H(z)$, which can be written as:

$$H_\varepsilon(z) = \frac{1}{2}\left|1 + \frac{2}{\pi}\arctan\left|\frac{z}{\varepsilon}\right|\right| \;, \varepsilon \to 0. \tag{24}$$

The regularized approximation $\delta_\varepsilon(z)$ of Dirac delta function $\delta_0(z)$ is correspondingly computed by:

$$\delta_\varepsilon(z) = \frac{1}{\pi} \cdot \frac{\varepsilon}{\varepsilon^2 + z^2}. \tag{25}$$

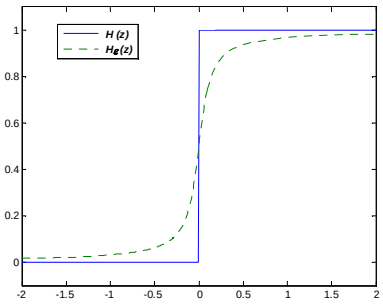

Figure 3: Heaviside function $H(z)$ and its regularized approximation $H_\varepsilon(z)$.

However, with the approximation of the Heaviside function, the energy functional defined in (21) has no minimizer ϕ at all [Lee, 06]. Even after the curve stops evolving, the value of $\phi(x, y)$ (on both sides of the curve) keeps moving to $+\infty$ or

$-\infty$. Due to the continual increase in the magnitude of the value of $\phi(x, y)$, it becomes difficult to set a termination criterion for curves evolution. Therefore, this problem is usually solved by setting a threshold for iteration time in advance. Curve evolves for a number of iterations assuming that the true boundaries will be obtained at the end of the process. However, there are few possible problems associated with this form of termination criterion, particularly when a large threshold is used. For instance, the true boundaries might have been obtained long before the iteration process ends. Thus, a lot of computational resources are wasted, which will increase the execution time unnecessarily. Moreover, if the iteration process is continued for a long time, the results might be unsatisfactory because of some abnormal noise points existing near the true boundaries.

In our multi-layer level set method, curve will evolve in not only one image layer. Therefore, we cannot run the iteration process for an insufferable long time in a single image layer and should also prevent the curve from stopping this process prematurely. Thus, we consider establishing the termination criterion based on the change of energy.

In (20), if $\lambda_1 = \lambda_2 = 1$, the second and third item of energy functional can be called as fitting term [Chan, 01]:

$$F_1(C_l) + F_2(C_l) = \int\limits_{inside(C_l)} \left|L_l(x, y) - c_1\right|^2 dxdy + \int\limits_{outside(C_l)} \left|L_l(x, y) - c_2\right|^2 dxdy . \tag{26}$$

It's obviously seen that the fitting term keeps decreasing while the curve evolves towards the true boundaries of one class of object in a certain image layer L_l, and the true boundaries C_l^* is the minimizer of the fitting term.

$$\inf_{C_l}(F_1(C_l) + F_2(C_l)) \approx 0 \approx F_1(C_l^*) + F_2(C_l^*) . \tag{27}$$

Therefore, we can approximately obtain the energy minimization value by:

$$\inf_{c_1, c_2, C_l}(E_l^{ML}(c_1, c_2, C_l)) \approx \mu Length(C_l^*) . \tag{28}$$

Actually, (28) can be the termination criterion for curves evolution. But, it can't be directly implemented in practice because of its approximate equal sign. In our numerical solution, we use another form of this termination criterion by determining the length of evolving curve $Length(C_l(t))$ at each iteration. When curve reaches the true boundary, it is obvious that the variable $Length(C_l(t))$ will remain almost constant. Here, we give the termination criterion for the curve evolution in a single image layer:

Termination criterion: *If the absolute value of the change of the curve length* $\left|Length(C_l(t)) - Length(C_l(t-1))\right|$ *remains smaller than a given threshold* ξ_{length} *over a fixed threshold of iterations uct , the evolution of curve in the lth image layer will be stopped.*

The pseudocode of this termination criterion is listed as follows:

$st = 1;$
… …
if $\left|Length(C_l(t)) - Length(C_l(t-1))\right| \le \xi_{length}$ *then*
{ *if* $st == uct$ *then stop evolution of curve*;
$st = st + 1;$
} *else* $st = 1;$
end

If the condition $\left|Length(C_l(t)) - Length(C_l(t-1))\right| \le \xi_{length}$ is firstly satisfied at a later stage, we do not stop the evolution of curve immediately. Instead, we examine whether or not the condition is maintained over a fixed threshold of iterations *uct* before stopping the evolution of curve. This examination must be performed because the evolution process often slows down temporarily even before true boundary is reached. In practice, the choice of two thresholds is flexible. Generally, we set $uct = 10$ and $\xi_{length} = 5$.

3.5 Adaptive Improvement of Curve Evolution Speed

In our multi-layer level set method, curve within each image layer always evolves from the same initial position. The curve evolution may slow down gradually since the initial curve may become far from the objects in subsequently obtained image layers. Therefore, we consider speeding up the curve evolution process in subsequent image layers.

We can approximate the solution of differential equation in the continuous domain defined in (23a) by a finite difference scheme as follows:

$$\begin{aligned}\frac{\phi_{i,j}^{n+1} - \phi_{i,j}^{n}}{\Delta t} = \delta_\varepsilon(\phi_{i,j}^n)\Bigg[& \frac{\mu}{h^2}\Delta_-^x \cdot \left(\frac{\Delta_+^x \phi_{i,j}^{n+1}}{\sqrt{(\Delta_+^x \phi_{i,j}^n)^2/(h^2) + (\phi_{i,j+1}^n - \phi_{i,j-1}^n)^2/(2h)^2}}\right) \\ & + \frac{\mu}{h^2}\Delta_-^y \cdot \left(\frac{\Delta_+^y \varphi_{i,j}^{n+1}}{\sqrt{(\Delta_+^y \phi_{i,j}^n)^2/(h^2) + (\phi_{i+1,j}^n - \phi_{i\_1,j}^n)^2/(2h)^2}}\right) \\ & - \lambda_1 (L_{l,i,j} - c_1(\phi^n))^2 + \lambda_2 (L_{l,i,j} - c_2(\phi^n))^2 \Bigg]\end{aligned} \tag{29}$$

where Δt is time-step, h is grid spacing, $\Delta_-^x \phi_{i,j} = \phi_{i,j} - \phi_{i-1,j}$, $\Delta_+^x \phi_{i,j} = \phi_{i+1,j} - \phi_{i,j}$, $\Delta_-^y \phi_{i,j} = \phi_{i,j} - \phi_{i,j-1}$, $\Delta_+^y \phi_{i,j} = \phi_{i,j+1} - \phi_{i,j}$. In this paper, the regularized approximation $\delta_\varepsilon(z)$ of Dirac delta function $\delta_0(z)$ is computed by (25).

It can be deduced from (29) that the value of Δt has a certain influence on the evolving speed, and a larger time-step Δt can speed up the curve evolution process. We implemented the difference scheme of (29) with different Δt's. It can be observed that, for small values of Δt, though the curve evolution was slow, the curve evolution results were satisfactory. When larger time-steps were used to speed up the evolution process, we sometimes got inaccurate results in one image layer. Therefore, the minor errors will be kept accumulated in subsequent image layers, which can cause the solution to go haywire. To keep the stability of our method, we try to modify some

other controlling variables to speed up the curve evolution process instead of the time-step Δt.

The first controlling variable we selected is grid spacing h. In level set method, the curve is generally described implicitly as the zero level set function and discretized on a uniform Cartesian grid [Engquist, 05]. The grid point (i, j) is corresponding to each pixel in image layer if the value of h is 1. With the increase of the value of h, the number of pixels which need to be computed decreases accordingly. As a result, the curve evolving speed can also be improved.

Since $\delta_\varepsilon(z)$ is commonly represented on the computational grid, the regularization parameter ε is relative to the grid spacing h with $\varepsilon = \alpha h$ ($1 \le \alpha \le 2$). Therefore, we selected the regularization parameter ε as the second controlling variable. Further, $\delta_\varepsilon(z)$ can be replaced by $\delta_h(z)$ if we set $\alpha = 1$.

$$\delta_h(z) = \frac{1}{\pi} \cdot \frac{h}{h^2 + z^2}. \tag{30}$$

By modifying the values of h and ε, we successfully speed up the curve evolution process. However, curves may sometimes stop evolving before they reach the true boundaries of objects in one image layer and produce the unsatisfactory results in subsequent image layers. The reason is that the threshold of iterations *uct* in termination criterion described in Section 3.4 is always identical in each image layer, assuming that the evolving speed also maintains constant. Since the speed of curve evolution increases, the value of *uct* should also be increased accordingly.

In this paper, we employ three controlling variables to improve the curve evolution speed, which are grid spacing h, regularization parameter ε and threshold of iterations *uct*. As described in Section 3.1, the intensity difference in each image layer decreases gradually from original image layer L_0 to background image layer L_n. Here, we computed the ratio of difference between the maximum and minimum intensities of pixel in original image layer L_0 and current image layer as a scaling parameter. Thus, the values of three controlling variables can be adaptively modified based on the scaling parameter and a given increment of each controlling variable before curve evolves in each image layer except in original image layer L_0 and background image layer L_n. Thus, the modifying scheme is defined as follows:

$$\begin{cases} h(l) = h(0) + \dfrac{I_{\max}(0) - I_{\min}(0)}{I_{\max}(l) - I_{\min}(l)} \times \Delta h \\ \varepsilon(l) = \alpha \cdot h(l) \\ uct(l) = uct(0) + \dfrac{I_{\max}(0) - I_{\min}(0)}{I_{\max}(l) - I_{\min}(l)} \times \Delta uct \end{cases}, \quad l = 1, 2, \ldots n-1, \tag{31}$$

where $h(0)$ and $uct(0)$ are the values of h and *uct* in original image layer L_0, respectively. $h(l)$, $\varepsilon(l)$ and $uct(l)$ are the values of h, ε and *uct* in the *lth* image layer L_l, respectively. $I_{\max}(0)$ and $I_{\min}(0)$ are the maximum and minimum intensities of pixel in L_0, respectively. $I_{\max}(l)$ and $I_{\min}(l)$ are the maximum and

minimum intensities of pixel in L_l, respectively. Δh and Δuct are the increments of h and uct. α is the scaling of ε relative to h. Usually, we set $0 \le \Delta h \le 1, 1 \le \Delta uct \le 5, \alpha = 1.0$ or 1.5.

3.6 Detection of Background Image Layer

As mentioned in Section 3.1, our multi-layer level set evolution procedure should be terminated if background image layer $L_{background}$ (L_n) is reached. It seems to easily detect that background image layer is reached if the object class number n is confirmed before algorithm starts. However, we can hardly estimate the value of n in a given image since it is always a difficult problem in image processing. Even if this problem can be solved by using some new image processing techniques, the requirement of a much long time for pre-processing seems to be unacceptable for this method. In this paper, we will give an easily implemented and efficient criterion to judge whether background image layer is reached or not.

From the definition of background image layer $L_{background}$ in (15), we can know that $L_{background}$ does not contain any objects, in other words, no true boundaries exist in $L_{background}$. If the curve still starts evolving from the initial position, it should finally evolve into a pixel point according to the energy minimization formula in (28) since C_l^* does not exists.

$$\inf_{c_1, c_2, C_n} (E_n^{ML}(c_1, c_2, C_n)) \approx \mu Length(pixel) = \mu, \tag{32}$$

where *pixel* denotes a evolving convergence point in $L_{background}$. However, this evolution process from curve to a pixel point will take a very long time for most of images. Therefore, we consider detecting whether or not $L_{background}$ is reached before curve starts evolving.

Actually, it should be noticed that the value of fitting term in (26) maintains near zero in the whole level set evolution from curve to a pixel point in $L_{background}$.

$$\begin{cases} c_1 \approx c_2 \\ F_1(C_n) + F_2(C_n) \approx 0 \end{cases}. \tag{33}$$

Thus, the minimization of the fitting term in (27) is already achieved before curve starts evolving in $L_{background}$.

$$\inf_{C_n} (F_1(C_n) + F_2(C_n)) \approx F_1(C_I) + F_2(C_I) \approx 0, \tag{34}$$

where C_I is curve in initial position.

Here, we proposed a criterion to judge whether or not background image layer is reached by comparing the average of $F_1(C_I)$ with a given average energy threshold θ before curve starts evolving in each image layer L_l:

$$\frac{1}{V}F_1(C_I)=\frac{1}{V}\int_{inside(C_I)}\left|L_l(x,y)-c_1\right|^2 dxdy \begin{cases} > \\ < \end{cases} \theta \begin{cases} L_{background} \text{ is not reached} \\ L_{background} \text{ is reached} \end{cases}, \quad (35)$$

where V is the number of pixels inside C_I, l denotes image layer index. Usually, we set the average energy threshold $0<\theta<0.5$.

Now, we can describe the steps of our multi-layer level set method as follows:

Step 1. Input original image (layer) L_0, set image layer index $l=0$;

Step 2. Set initial curve C_I in L_0. Set the value of time step Δt and the length parameter μ in (29). Set the value of $h(0)$, $uct(0)$, α, Δh, Δuct in (31). Set the value of average energy threshold θ in (35);

Step 3. Use fast marching method to construct the sign map S. Compute $dist((x,y),C_I)$ using Voronoi source scanning method. Construct the level set function φ by multiplying $dist((x,y),C_I)$ by corresponding S_{ij} in S;

Step 4. Judge whether $L_{background}$ is reached or not according to (35). If $L_{background}$ is reached, the algorithm is stopped; otherwise, go to next step;

Step 5. Move level set function φ to a steady state according to (23). Meanwhile, the curve C_l (zero level set function) evolves towards the true boundaries of the *lth* class of object and finally stops evolving based on the termination criterion described in Section 3.4.

Step 6. Replace the intensities of the *lth* class of object regions $\Omega_l^1 \cup \Omega_l^2 \cup \cdots \cup \Omega_l^{l_m}$ by an average of intensity of the outer regions to form a new image layer L_{l+1};

Step 7. Modify the values of $h(l+1)$, $\varepsilon(l+1)$ and $uct(l+1)$ according to (31), $l=l+1$. Return to *Step* 4.

4 Experimental Results

In this Section, we present the experimental results of our multi-layer level set method on some real and synthetic images. The proposed method was implemented on a computer with Intel Pentium 2.6GHz CPU, 512M RAM, and Windows XP operating system.

Though our method is designed for multi-phase image segmentation, it can still be applied to segment the two-phase image. Figs.4 (b)-(d) show the segmentation of a two-phase noisy image using the multi-layer level set method. The robustness property of our method is inherited from Chan-Vese model. The irregular initial curve is shown in Fig.4 (b). Afterwards, the curve splits into several curves according to the topological structure of objects in original image layer (as shown in Fig.4 (c)). Finally, the evolving curves stop on the true boundary of each object after 54 iterations, as can be seen in Fig.4 (d). The background image layer L_1 is shown in Fig.4 (e). The proposed termination criterion for curve evolution in a single image layer also takes effect on two-phase image. It can be seen from Fig.4 (f) that the

length of evolving curve increases rapidly while the curve starts splitting at initial iterations and maintains constant after 44 iterations ($uct = 10$).

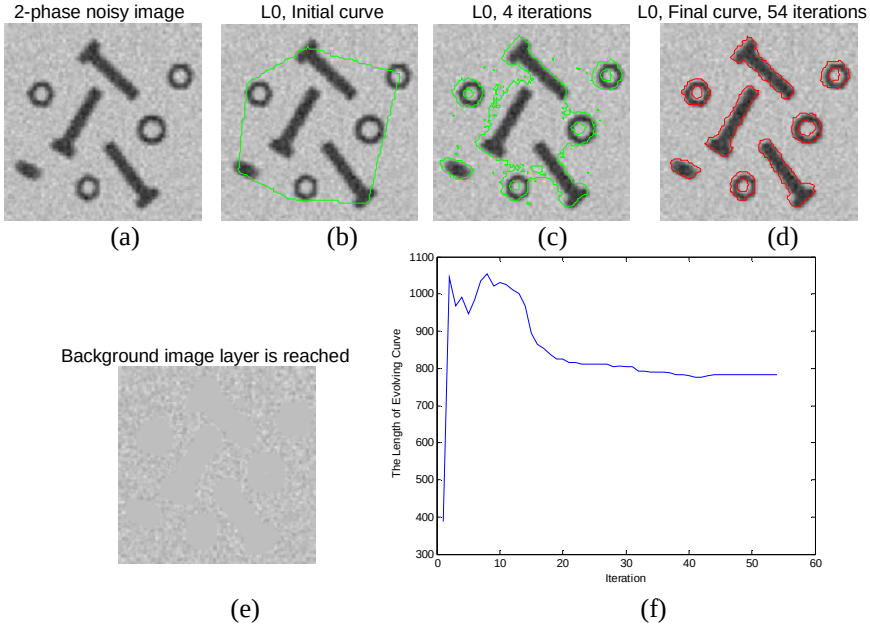

Figure 4: Two-phase noisy image segmentation. (a) 2-phase noisy image; (b) Initial curve; (c) Intermediate result after 4 iterations; (d) Final segmentation result after 54 iterations in L_0 *; (e) Background image layer* L_1 *; (f) Length change of evolving curve.* $Size = 100 \times 100$, $\Delta t = 0.1$, $\mu = 0.01 \cdot 255^2$, $\theta = 0.1$, $h = 1$, $uct = 10$, $\alpha = 1$.

Figs.5 (b)-(g) illustrate the segmentation of a synthetic three-phase image using our proposed method. The irregular initial curve is shown in Fig.5 (b), which touches each object. Fig.5 (c) shows that initial curve splits into two curves after 20 iterations. As can be seen in Fig.5 (d), the evolving curves stop on true boundaries of the 1*st* class of objects with smaller intensities after 41 iterations. New image layer L_1 is formed by replacing the intensities of the 1*st* class of objects with the average of intensities of outer regions. Then, the curve returns to its initial position and continue to evolve in L_1 (as shown in Fig.5 (e)). Afterwards, the curve still starts splitting in L_1 , as can be seen in Fig.5 (f)). Fig.5 (g) shows that the evolving curves stop on the true boundaries of the 2*nd* class of objects with higher intensities after 81 iterations. Then, background image layer L_2 is formed in the same way like L_1 (as shown in Fig.5 (h)). Fig.5 (i) is the length changing curve of the evolving curves in L_0 and L_1 . Fig.5 (j) shows the average of $F_1(C_I)$ before the curve evolution in each image layer. The average of $F_1(C_I)$ in L_2 is 0.0684 which is smaller than the given threshold

$\theta = 0.1$, and it shows that the proposed termination criterion for whole evolution procedure takes effect.

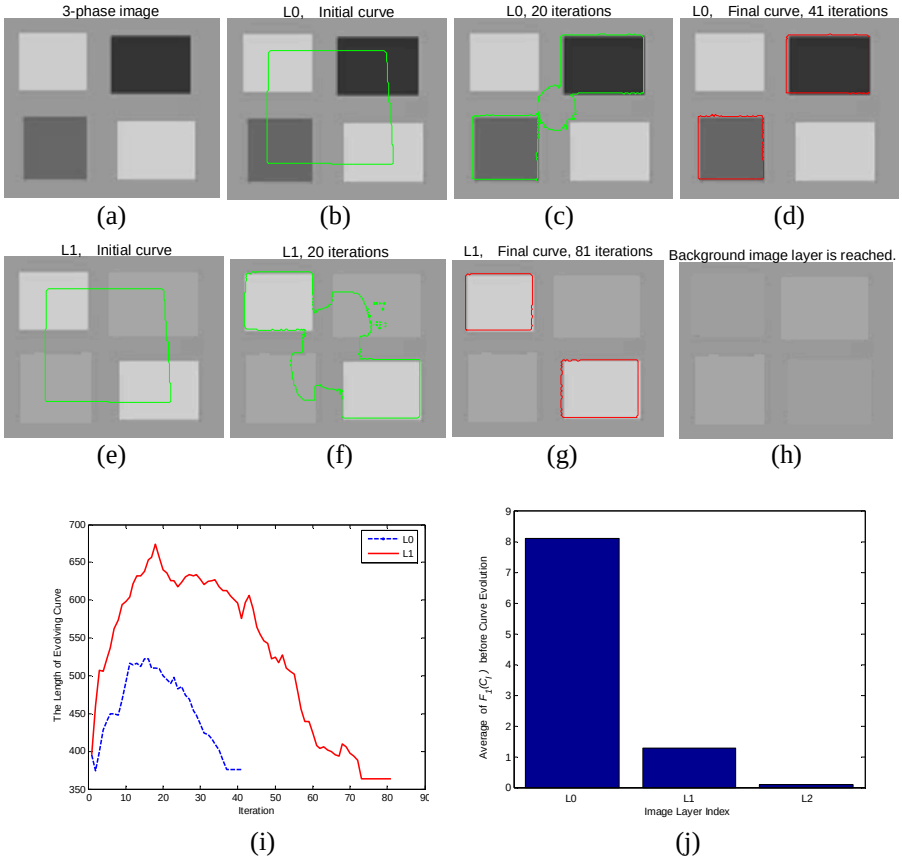

Figure 5: Synthetic three-phase image segmentation using proposed method. (a) Synthetic 3-phase image; (b) Initial curve in L_0; (c) Intermediate result after 20 iterations in L_0; (d) Segmentation result after 41 iterations in L_0; (e) Initial curve in L_1; (f) Intermediate result after 20 iterations in L_1; (g) Segmentation result after 81 iterations in L_1; (h) Background image layer L_2; (i) Length change of evolving curves in L_0 and L_1; (j) Average of $F_1(C_I)$ before curve evolution. Size= 150×124, $\Delta t = 0.1$, $\mu = 0.01 \cdot 255^2$, $\theta = 0.1, h(0) = 1, uct(0) = 5, \alpha = 1, \Delta h = 0.5, \Delta uct = 2$.

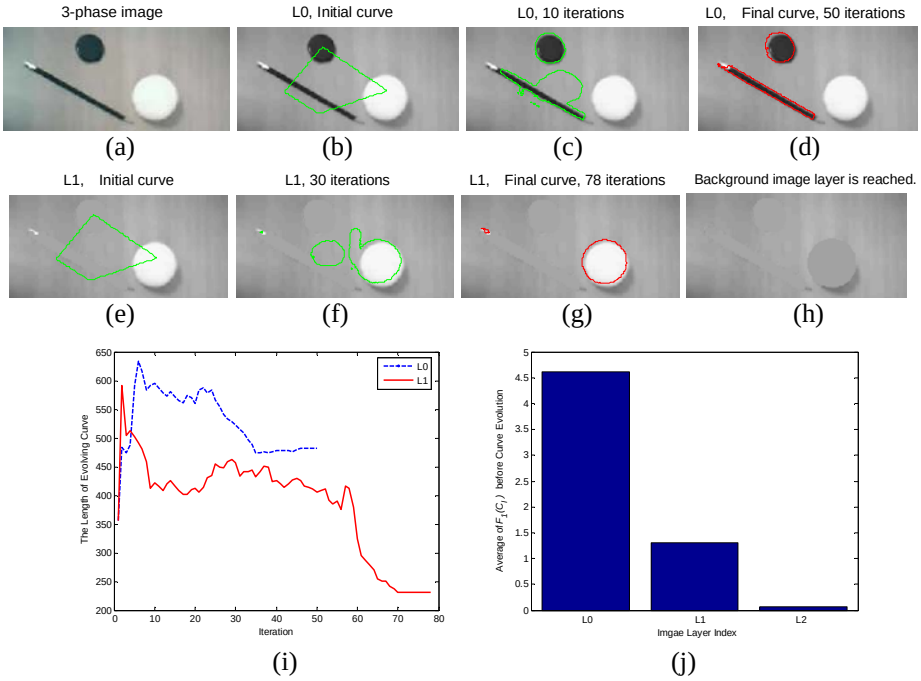

Figure 6: Real three-phase image segmentation using our proposed method. (a) Real 3-phase image; (b) Initial curve in L_0; (c) Intermediate result after 10 iterations in L_0; (d) Segmentation result after 50 iterations in L_0; (e) Initial curve in L_1; (f) Intermediate result after 30 iterations in L_1; (g) Segmentation result after 78 iterations in L_1; (h) Background image layer L_2; (i) Length change of evolving curve in L_0 and L_1; (j) Average of $F_1(C_1)$ before curve evolution. Size= 250×119, $\Delta t = 0.1$, $\mu = 0.01\cdot 255^2$, $\theta = 0.1$, $h(0)=1, uct(0)=5, \alpha=1, \Delta h = 0.5, \Delta uct = 2$.

The performance of our proposed method for a real three-phase image is illustrated in Fig.6. The irregular initial curve touching each object is shown in Fig.6 (b). It should be noticed that the body and accessory rubber of pencil in given image belong to two phases. Fig.6 (c) shows the intermediate result that initial curve successfully splits into two curves according to topological structure of pencil body and black checker. After 50 iterations, curves stop evolving on true boundaries of pencil body and black checker, as can be seen in Fig.6 (d). New image layer L_1 is formed by replacing the intensities of pencil body and black checker with the average of intensities of outer regions. Afterwards, the curve returns to its initial position and continues to evolve in L_1 (as shown in Fig.6 (e)). Fig.6 (f) shows that the curve splits in L_1. Finally, curves stop evolving on true boundaries of accessory rubber of pencil and white ping-pang ball after 78 iterations (as illustrated in Fig.6 (g)). Background

image layer L_2 is shown in Fig.6 (h). Fig.6 (i) shows the length change of the evolving curves in L_0 and L_1. The average of $F_1(C_I)$ before curve evolution in each image layer is shown in Fig.6 (j).

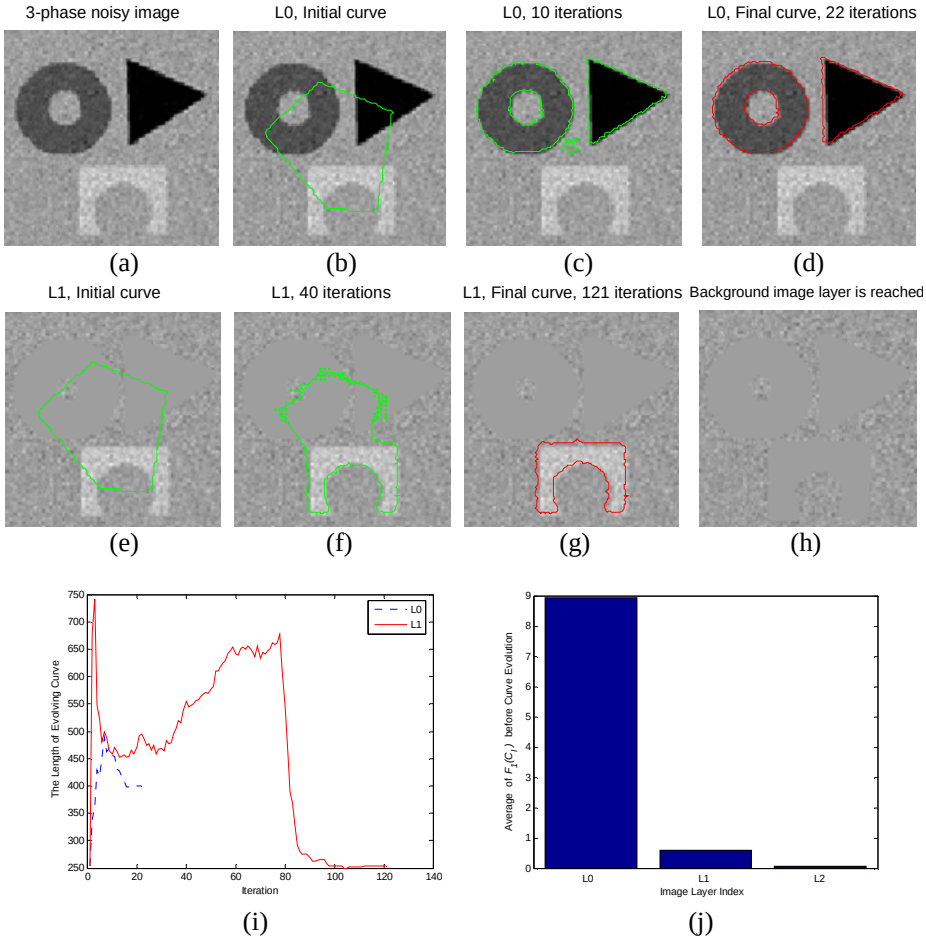

Figure 7: Synthetic three-phase noisy image segmentation using proposed method. (a) Synthetic 3-phase noisy image; (b) Initial curve in L_0; (c) Intermediate result after 10 iterations in L_0; (d) Segmentation result after 22 iterations in L_0; (e) Initial curve in L_1; (f) Intermediate result after 40 iterations in L_1; (g) Segmentation result after 121 iterations in L_1; (h) Background image layer L_2; (i) Length change of evolving curves in L_0 and L_1; (j) Average of $F_1(C_I)$ before curve evolution. Size=100×100, $\Delta t = 0.1$, $\mu = 0.01\cdot 255^2$, $\theta = 0.1$, $h(0) = 1$, $uct(0) = 5$, $\alpha = 1$, $\Delta h = 0.5$, $\Delta uct = 2$.

Fig.7 (b)-(g) illustrate the segmentation process of a synthetic three-phase noisy image from [Vese, 02] using our method. Background image layer L_2 is shown in Fig.7 (h). Fig.7 (i) shows the length change of the evolving curves in L_0 and L_1. The average of $F_1(C_I)$ before curve evolution in each image layer is shown in Fig.7 (j). The total segmentation time is 13.67 seconds. Readers can refer to [Vese, 02] for segmentation results using multi-phase Chan-Vese method.

Here, we also used multi-phase Chan-Vese method to segment the same three-phase images shown in Fig.5 (a) and Fig.6 (a). Two coupled level set functions are employed for evolution according to (9) and (10). Two un-overlapped circles are selected as initial curves, as can be seen in Fig.8 (a) and (e). As a result, multi-phase Chan-Vese method can segment only one object after a lot of iterations (as shown in Fig.8 (d)). The reason for why the segmentation task failed is mostly due to the cross topological structure of objects which causes a slow convergence and even makes two level set functions evolve to a possibly wrong direction. Another three-phase image in Fig.6 (a) was successfully segmented after 100 iterations using multi-phase Chan-Vese method.

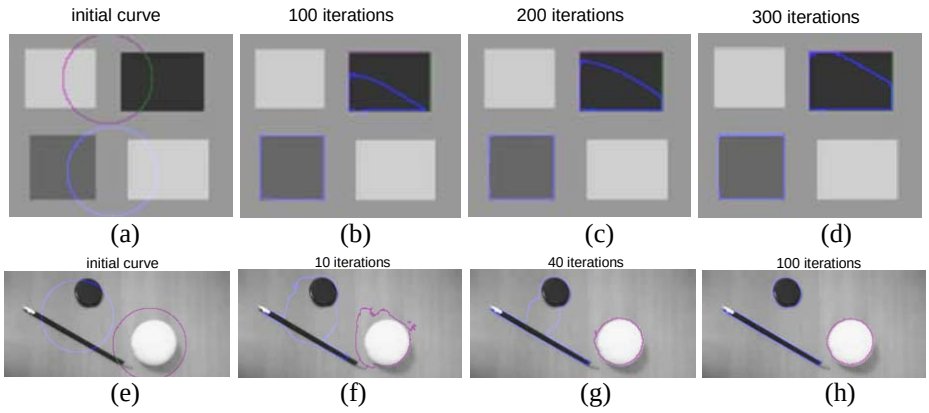

Figure 8: Segmentation using multi-phase Chan-Vese method. (a) Initial curves; (b) Intermediate result after 100 iterations; (c) Intermediate result after 200 iterations; (d) Intermediate result after 300 iterations; (e) Initial curves; (f) Intermediate result after 10 iterations; (g) Intermediate result after 40 iterations; (h) Segmentation result after 100 iterations. $\Delta t = 0.1$, $\mu = 0.01 \cdot 255^2$, $h = 1$, $\varepsilon = 1$.

Table 1 shows the performance comparisons of segmenting Fig.5 (a) and Fig.6 (a) using multi-phase Chan-Vese method and our proposed multi-layer level set method. It can be seen from Table 1 that the difference of the initialization time for two methods is very small since Voronoi source scanning method is used to compute signed distance function in our method which can greatly decrease the overall computational complexity. Unlike multi-phase Chan-Vese method, our method needs only one level set function, which avoids complicated evolution equations for multi-phase images. Thus, the segmentation time of our method is obviously smaller than that of multi-phase Chan-Vese method. Moreover, multi-phase Chan-Vese method

sometimes shows unsuitability for those images with complicated distributing topological structure like Fig.5 (a). Particularly, it can be seen that our method requires that the initial curve be close to or touch all objects as much as possible. Obviously, the requirement for the initial curve of our method can be easily satisfied. Notice that the image segmentation needs to be made much more efficiently and widely used for various images with different topological structures in practice. Thus, our method is a more preferred candidate for practical image segmentation than multi-phase Chan-Vese method for it can not only reduce the time consumed but also easily converge within a limited number of iterations.

	Fig 5 (a), Size=150×124		
	Successful Segmentation	Initialization Time (s)	Segmentation Time (s)
Multi-phase Chan-Vese Method	No	0.203	118.68
Multi-layer Level Set Method	Yes	0.418	18.53
	Fig 6 (a), Size= 250×119		
	Successful Segmentation	Initialization Time (s)	Segmentation Time (s)
Multi-phase Chan-Vese Method	Yes	0.234	48.62
Multi-layer Level Set Method	Yes	0.769	27.55

Table 1: The performance comparisons of segmenting Fig.5 (a) and Fig.6 (a) using multi-phase Chan-Vese method and our proposed multi-layer level set method.

5 Conclusions

In this paper, we proposed a novel multi-layer level set method for solving the multi-phase image segmentation problem. Our method successfully extends single level set method to multi-phase image segmentation by introducing the conception of image layer into level set method as well as adopting a hierarchical form. In addition, in our proposed method, some modifications were also made to the numerical solution of bimodal Chan-Vese model. New initialization method and computing method of signed distance function using fast marching method and Voronoi source scanning method were introduced. To ensure that the curve can automatically stop evolving in a single image layer, a termination criterion based on the length of the evolving curve was proposed. A speeding up scheme was designed for curve evolution in a queue of sequential image layers. In particular, an easily implemented termination criterion was proposed for the whole evolution procedure, which is satisfied when the background image layer is reached. Finally, the experimental results show that our method works well while segmenting multi-phase images and is also robust to noise.

Moreover, compared with multi-phase Chan-Vese method, our method has a less time-consuming computation and much faster convergent speed.

Acknowledgements

This work was supported by the grants of the National Science Foundation of China, Nos. 60772130 & 60705007 & 30700161, the grant from the National Basic Research Program of China (973 Program), No.2007CB311002, the grants from the National High Technology Research and Development Program of China (863 Program), Nos. 2007AA01Z167 & 2006AA02Z309, the grant of the Guide Project of Innovative Base of Chinese Academy of Sciences (CAS), No.KSCX1-YW-R-30, the grant of Oversea Outstanding Scholars Fund of CAS, No.2005-1-18, the grant of the Graduate Students' Scientific Innovative Project Foundation of CAS, the grant of the Scientific Research Foundation of Education Department of Anhui Province, No. KJ2007B233, the grant of the Young Teachers' Scientific Research Foundation of Education Department of Anhui Province, No. 2007JQ1152 and the grant of the Scientific Research Foundation of Hefei University, No. 06KY007ZR.

References

[Adams, 94] Adams, R. and Bischof, L.: Seeded region growing, *IEEE Trans. Pattern Anal. Mach. Intell.*, 16(6): 641-647, Jun. 1994.

[Allaire, 05] Allaire, G. and Jouve, F. A.: A level-set method for vibration and multiple loads structural optimization, *Comput. Meth. Appl. Mech. Eng.*, 194: 3269-3290, 2005.

[Chan, 01] Chan, T. F. and Vese, L. A.: Active contours without edges, *IEEE Trans. Image Process.*, 10(2): 266-277, Feb. 2001.

[Chang, 94] Chang, Y. and Li, X.: Adaptive image region-growing, *IEEE Trans. Image Process.*, 3(6): 868-872, Nov. 1994.

[Chaudhury, 07] Chaudhury, K. N. and Ramakrishnan, K. R.: Stability and convergence of the level set method in computer vision, *Pattern Recognition Letters.*, 28(7): 884-893, 2007.

[Engquist, 05] Engquist, B., Tornberg, A.K. and Tsai, R.: Discretization of Dirac delta functions in level set methods, *J. Comput. Phys.*, 207(1): 28-51, 2005.

[Hijjatoleslami, 98] Hijjatoleslami, S. A. and Kitter, I.: Region growing: a new approach, *IEEE Trans. Image Process.*, 7(7): 1079-1084, Jul. 1998.

[Jeon, 05] Jeon, M., Alexander, M., Pedrycz, W. and Pizzi, N.: Unsupervised hierarchical image segmentation with level set and additive operator splitting, *Pattern Recognition Letters.*, 26: 1461-1469, 2005.

[Kass, 87] Kass, M., Witkin, A. and Terzopoulos, D.: Snakes: Active contour models, *Int. J. Comput. Vision.*, 1(4): 321-331, 1987.

[Lee, 06] Lee, S. H. and Seo, J. K.: Level set-based bimodal segmentation with

stationary global minimum, *IEEE Trans. on Image Process*., 15(9): 2843-2852, 2006.

[Linda, 01] Linda, G. S. and George, C. S.: *Computer Vision.*, New Jersey: Prentice-Hall, 2001.

[Lin, 90] Lin, Y. W. and Lee, S. U.: On the color image segmentation algorithm based on the thresholding and the fuzzy C-means techniques, *Pattern Recognition*., 23(9): 935-952, 1990.

[Malladi, 95] Malladi, R., Sethian, J. A. and Vemuri, B .C.: Shape modeling with front propagation: A level set approach, *IEEE Trans. Pattern Anal. Mach. Intell*., 17(2): 158-175, 1995.

[Mumford, 89] Mumford, D. and Shah, J.: Optimal approximation by piecewise smooth functions and associated variational problems, *Commun. Pure Appl. Math*., 42: 577-685, 1989.

[Osher, 88] Osher, S. and Sethian, J. A.: Fronts Propagating with Curvature-Dependent Speed: Algorithms Based on Hamilton-Jacobi Formulations, *J. Comput. Phys*., 79(1): 12-49, 1988.

[Palmer, 96] Palmer, P. L., Dabis, H. and Kitler, J.: A performance measure for boundary detection algorithms, *Computer Vision and Image Understanding*., 63(3): 476-494, 1996.

[Sethian, 96] Sethian, J. A.: *Level set methods and fast marching methods*., Cambridge University Press, 1996.

[Shi, 00] Shi, J. and Malik, J.: Normalized cuts and image segmentation, *IEEE Trans. Pattern Anal. Mach. Intell*., 22(8): 888-905, Aug. 2000.

[Sonka, 02] Sonka, M., Hlavac, V. and Boyle, R.: *Image Processing, Analysis and Machine Vision, Second Edition*., Beijing: Posts & Telecom Press, 2002.

[Towers, 07] Towers, J.: Two methods for discretizing a delta function supported on a level set, *J. Comput. Phys*., 220: 915-931, 2007.

[Tsai, 01] Tsai, A., Yezzi, A. and Willsky, A. S.: Curve evolution implementation of the Mumford-Shah functional for image segmentation, denoising, interpolation, and magnification, *IEEE Trans. Image Process*., 10(8): 1169-1186, 2001.

[Tsai, 02] Tsai, Y. H.: Rapid and accurate computation of the distance function using grids, *J. Comput. Phys*., 178(1): 175-195, 2002.

[Tsai, 05] Tsai, Y. H. and Osher, S.: Total Variation and Level Set Based Methods in Image Science, *Cambridge University Press, Acta Numerica*., 1-61, 2005.

[Urquhart, 82] Urquhart, R.: Graph theoretical clustering based on limited neighborhood sets, *Pattern Recognition*., 15(3): 173-187, 1982.

[Vese, 02] Vese, L. A. and Chan, T. F.: A multiphase level set framework for image segmentation using the Mumford and Shah Model, *Int. J. Comput. Vision*., 50(3): 271-293, 2002.

[Weber, 03] Weber, M., Blake, A. and Cipolla, R.: Initialisation and termination of active contour level-set evolutions, *In Proc. 2nd IEEE workshop on Variational, Geometric and Level Set Methods in Computer Vision*., 161-168, 2003.

[Xu, 98] Xu, C. and Prince, J. L.: Snakes, shapes, and gradient vector flow, *IEEE Trans. Image Process*., 7(3): 359-369, Mar. 1998.

[Yang, 02] Li, J., Yang, X. and Shi, P. F.: A fast level set approach to image segmentation based on Mumford-Shah model, *Chinese Journal of Computers*., 25(11): 1175-1183, 2002.